Presentation of new approach for energy consumption reduction with use of solar system

Alireza Latifi Sani[1] · M. Ayani[1] · S. Ali Behbahani-Nia[1] · Ahmad Shafee[2] · Houman Babazadeh[3,4]

Abstract

In hot and humid areas with high solar radiation intensity, the use of air conditioning systems on the basis of desiccant materials such as solar desiccant cooling systems with a view to reducing energy consumption and economic saving can be a good alternative to conventional air conditioning units. In this paper, in order to offer a cooling load of a sample space in the city of Bandar Abbas, which has a high latent load and high radiation intensity, solar absorption cooling cycle has been considered as the base cycle, and two absorption cooling cycles were designed for comparison. Then the three cycles were modeled in the TRNSYS software, studied technically and economically, and at the end the best cycle has been selected. In terms of current energy prices, application of solar energy in Iran is not economically feasible, so the solar absorption refrigeration cycle has been considered as the basic system for the cycle's comparison. Modeling of the expressed cycles was done in TRNSYS software. The basic cycle has been composed of two main parts of cooling by absorption chillers and providing the required heat supply by the solar collector, and also two desiccant dehumidification cycles have been added by a desiccant dehumidification system. In the economic analysis of the three systems, the costs estimation during lifetime (LCC) method also has been used. As a result of this modeling and due to the Act to amend energy prices, the cooling system with the help of desiccant wheel and using returned water of chiller's generator as the regeneration source, with an annual energy saving of about 29.1%, 29.1% (1,371,980 m^3) of natural gas consumption has been saved and the amount of 18/15% (156,667$) cost savings over 20 years compared to the base period, has been selected as the most efficient cooling system.

Keywords Solar cooling · Absorption chiller · Solar collector · Desiccant cooling

List of symbols

$\dot{Q}$	Heat transfer rate
T	Temperature
$\dot{m}$	Mass flow rate
h	Sensible enthalpy
$\tau\alpha$	Coefficient represents the effect of the pass
U_L	Overall heat loss coefficient
C_p	Specific heat capacity at constant pressure
I	Solar radiation intensity
A	Surface area
w	Humidity ratio
Capacity	Cooling capacity of the chiller
$\bar{T}$	The average air temperature
C_{min}	Minimum capacity
$f_{FullLoadCapacity}$	Fraction of the nominal load generated by the chiller
$f_{NominalCapacity}$	A fraction of the full load capacity
C_s	Initial cost
C_A	Price per square meter of collector area
C_v	Price per cubic meter of storage tank
V_s	Volume of tank
C_{aux}	The cost of fuel in auxiliary heater
C_g	Price per cubic meter of natural gas
L_v	Thermal value of natural gas
Q_{aux}	Energy from fuel

✉ Houman Babazadeh
  houman.babazadeh@tdtu.edu.vn

1 Department of Mechanical Engineering, K.N. Toosi University of Technology, Tehran, Iran

2 Institute of Research and Development, Duy Tan University, Da Nang 550000, Vietnam

3 Department for Management of Science and Technology Development, Ton Duc Thang University, Ho Chi Minh City, Vietnam

4 Faculty of Environment and Labour Safety, Ton Duc Thang University, Ho Chi Minh City, Vietnam

Introduction

In the recent years, population growth, economic development, the emergence of new industrialized countries and also the increase in the human's life quality have caused significant growth of energy consumption in the world like taking 10–20% of total electricity of the world by air conditioning systems [1]. The overall energy consumption disadvantages include non-renewable energy resource depletion, environmental pollution caused by emission of carbon monoxide (CO), changing weather patterns across the world, and reduction in the ozone layer thickness [2]. These factors have led many ways of renewable energy for cooling to be investigated widely. One of these solutions which is very reliable is the use of solar energy to produce part of the driving force required for cooling system whether compression or absorption. In the absorption cycles, the sun's energy is used to provide the required heat in generators; this heat content in single effect chillers is about 70–90 °C [3]. On the other hand, when the air conditioning system has to do dehumidification and reduce temperature simultaneously, the latent and sensible loads need to be separated so that they can be controlled effectively and precisely. In order to control and isolate latent load from sensible load in 1955, the desiccant cooling systems were introduced. Desiccant cooling systems through absorbing moisture in the desiccant material are able to separate latent and sensible loads and thus are promising to save energy and reduce emissions of greenhouse gases [4]. Through hybrid systems approach, many cycles can be introduced as a substitute for air conditioning purposes. One of these units is the solar desiccant absorption refrigeration cycle which employs solar energy to supply all or part of the required heat for chiller generator and desiccant regeneration section. Solar energy becomes popular these days [5–18]. Qin et al. [19] theoretically offers a new solution to balance the heat absorption of a built dam, a solution that is perhaps the most effective way to remedy the thermal asymmetry of a built-up dam.

Given the importance of this issue, many scientists today are researching and developing solar cooling systems, solar absorption cooling, desiccant cooling, and a combination of both of these. Fung et al. [20] examined five different cooling units for Hong Kong that included: solar electric condensing refrigeration, water absorption cooling, solar absorbing cooling (solid), mechanical refrigeration compression, and solid desiccant cooling, and concluded that the and solar absorption refrigeration systems and solar electric compression had the most energy savings. In terms of economic value of solar systems, it can also be expressed that the use of these systems can be quite economical by 2030 due to rising energy prices and a significant reduction in the production cost of solar collectors. In this field, Dieter Boyer et al. [21] to produce cooling demand with minimal cost and environmental impact have carried out an economic study and concluded that given the current prices of energy and non-financial support of governments, using the solar energy system has not been economical. In relation to the desiccant technology, Henning et al. [22] came to the conclusion that desiccant unit compared to conventional systems can contribute up to 50% energy savings. Moreover, such systems' operating costs are much lower and also more friendly with the environment. Daewoo et al. [23] demonstrated the viability of using desiccant cooling systems in various weather conditions was demonstrated and its benefits were significant in cost savings. Krishna and Mortti [24] conducted a test on the desiccant wheel containing Silica Gel and concluded with ambient air considered as process air left much impact on system performance. Vineyard et al. [25] compared desiccant system for harsh weather conditions and come to the conclusion that as the latent load share was greater in the total load, the desiccant system performance would be better. Performance of heat exchangers tried to be improved via researchers [26–44]. The purpose of current article was to calculate the technical and economic impact of adding desiccant wheel dehumidifier system to the common absorption cooling system. Due to the high humidity level of this project site, that is expected to have a positive effect. However, regarding extremely high radiation, solar hot water was utilized to supply hot water of chiller.

The purpose of this paper is to technically and economically examine the solar desiccant cooling system. Since typically the solar systems efficiency is not high, and using these systems for many functions and areas cannot be economical, therefore, as an innovation in this study and with the purpose of maximum efficiency of solar energy, to provide the required heat for desiccant wheel regeneration of hot H_2O returned from the chiller with a temperature of about 83 °C, which is primarily used to heat the regeneration air and then poured into the hot water storage tank and the collector. This will not only reduce support fuel consumption compared to the conventional hybrid cycles but also makes temperature of the water entering the collector drop; and this is expected to augment the efficiency of solar collector units.

Description systems

The sample that has been examined in this study is a single-story computer building with an area of 400 square meters in the city of Bandar Abbas which contains 150 people in peak condition. A weather condition at the project site is shown in Table 1.

Table 1 Weather information of the site

Latitude: 27.02°	Elevation: 33 feet
Winter dry bulb temperature: 45.5 °F	Winter wet bulb temperature: 42.5 °F
The maximum relative humidity of summer: 57.5%	The maximum humidity ratio of summer: 187.4 GR/LB
Summer dry bulb temperature: 105 °F	Summer wet bulb temperature: 89.47 °F
The maximum relative humidity of winter: 90%	The maximum humidity ratio of summer: 36 GR/LB
Indoor comfort temperature in summer: 20 °C	Indoor comfort humidity ratio: 0.008

Based on the above data and by HAP4.5 software, maximum cooling load in summer is 40 tons of refrigeration, total air discharge required is 16000cfm, and sensible heat ratio (SHR) is 0.473 for the building.

For the mentioned building cooling load, three hybrid cooling systems were considered and modeled in the TRNSYS software. The three systems were: solar absorption cooling cycle as basis cycle, solid desiccant cooling cycle combined with solar absorption cooling and direct air of regeneration, and solar desiccant absorption cooling cycle using heat returning of chiller generator for the regeneration as the original cycle that in the following each cycle components and method of operation will be discussed.
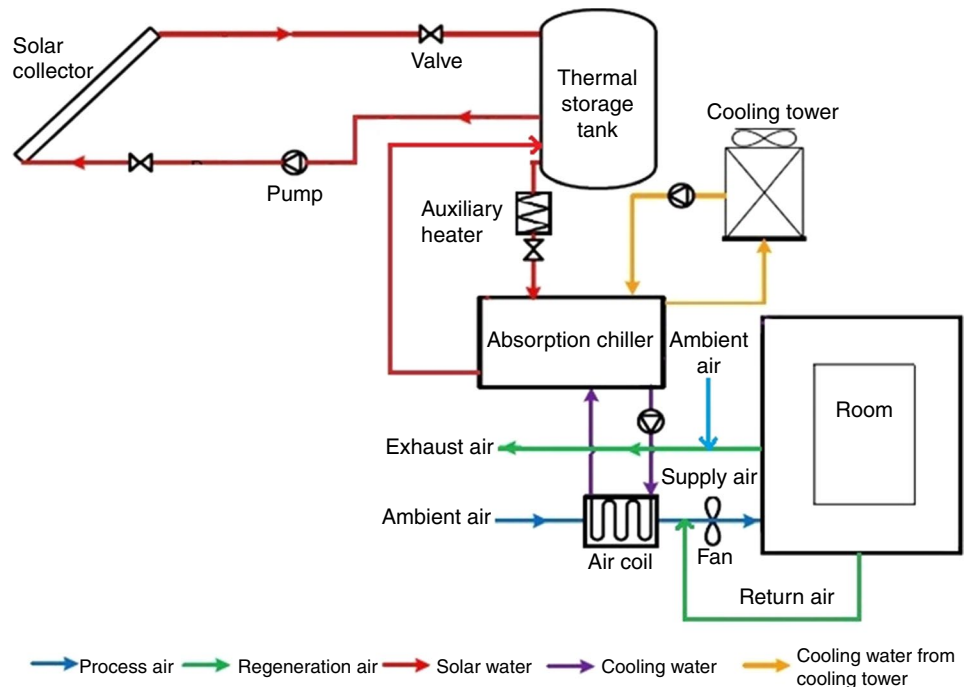
Solar absorption cooling cycles (basis cycle)

The cycle scheme is given in Fig. 1. As shown below, this cycle is composed of three main components: 1) the hot water supply required for chiller, 2) the cold water supply for cooling coils, and 3) the supply of interior comfort conditions by the air handling units.

Thus, each section contains a subset of components to meet the expected output of the sector. To get the required heat in the chiller generator, solar flat plate collectors have been applied. In order to ensure the required water temperature at all hours of the day, before a tank with auxiliary heater is used before chiller generator incoming. To provide the required cooling load in the cooling air, an air handling unit is used which in a cold water supply of a cooling coil is provided by an absorption chiller which is based on the load on the chiller and temperature of the returned water from coil into it deals with cold water supply with 7 °C temperature through heat absorption in generator.

Fig. 1 Solar absorption cycle scheme

Solid desiccant cooling cycle combined with solar absorption cooling and direct heating of air regeneration

In this sector due to high latent load and low sensible heat ratio, in order to save energy and increase thermal performance of the cooling cycle's equipments, a set of dehumidifiers like desiccant wheel are added to the previous cycle which contains three main parts of desiccant wheel, heat wheel, and direct heater of the returned air. Providing latent load supply is carried out by desiccant wheel with silica gel, and the schema of the cycle is shown in Fig. 2.

For continuous operation of desiccant wheel and doing dehumidification, in the desiccant material in dehumidification wheel are required to be retrieved after the stage of dehumidification, restore the moisture to the regeneration air and gets ready for next dehumidification. For the proper conduct of this process, the regeneration air must be heated to the proper level that as shown in Fig. 2, this heat is applied directly to the returned air by gas air heater.

Solar cooling absorption desiccant cycle using return heat of the chiller generator for the regeneration sector

The solar systems often have a low efficiency and are not cost-effective; one of the parameters affecting the efficiency of collector is the fluid temperature entering into it. On the other hand, temperature of the hot water returning from chiller generator is about 80–83 °C that is greater than the

needed temperature in this project is to restore the desiccant wheel. So as a useful and innovative solution, the output hot water from the chiller generator, as shown in Fig. 3, first needs to be entered in a water-to-air exchanger before the desiccant wheel and thereby the restoring water temperature gets to the required level. Then in the following, this water goes into the storage tank and from there goes into the collector with a temperature less than that in the previous cycle. After doing this, the external energy consumption is reduced and the collector efficiency and solar system are increased.

Systems modeling

To check the performance of each system and the influence of various parameters on the output conditions, the three above cycles are modeled based on Figs. 1–3 in the TRN-SYS software. Accordingly, in Fig. 4, the third version of the system (final system) can be seen in this application. In the above diagram, the type686 acts like a hypothetical building, and we enter the output of the carrier software in this type. Then, the output latent load of the type686 will be entered in type693. In the following, 60% of the output air of 693 and 40% of the total inflow from the ambient air enter into type648, and this type, based on the psychometric principles, mixes the two inputs and calculates the output air condition. Then the outlet air from the type648 enters into type506d, which has the function as air conditioner. The output air of type506d enters into type696, and it calculates the amount of transient heat.

Fig. 2 Schema of the solid desiccant cooling cycle combined with solar absorption cooling and direct heating of air regeneration
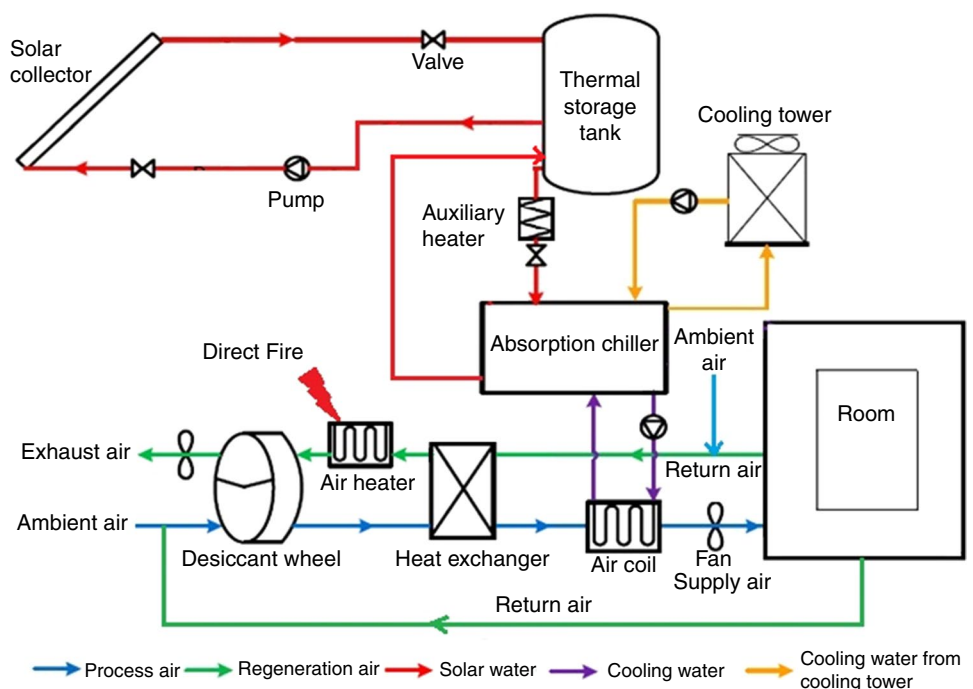
Fig. 3 Schema of the solar desiccant absorption cooling cycle using chiller generators return heat for regeneration
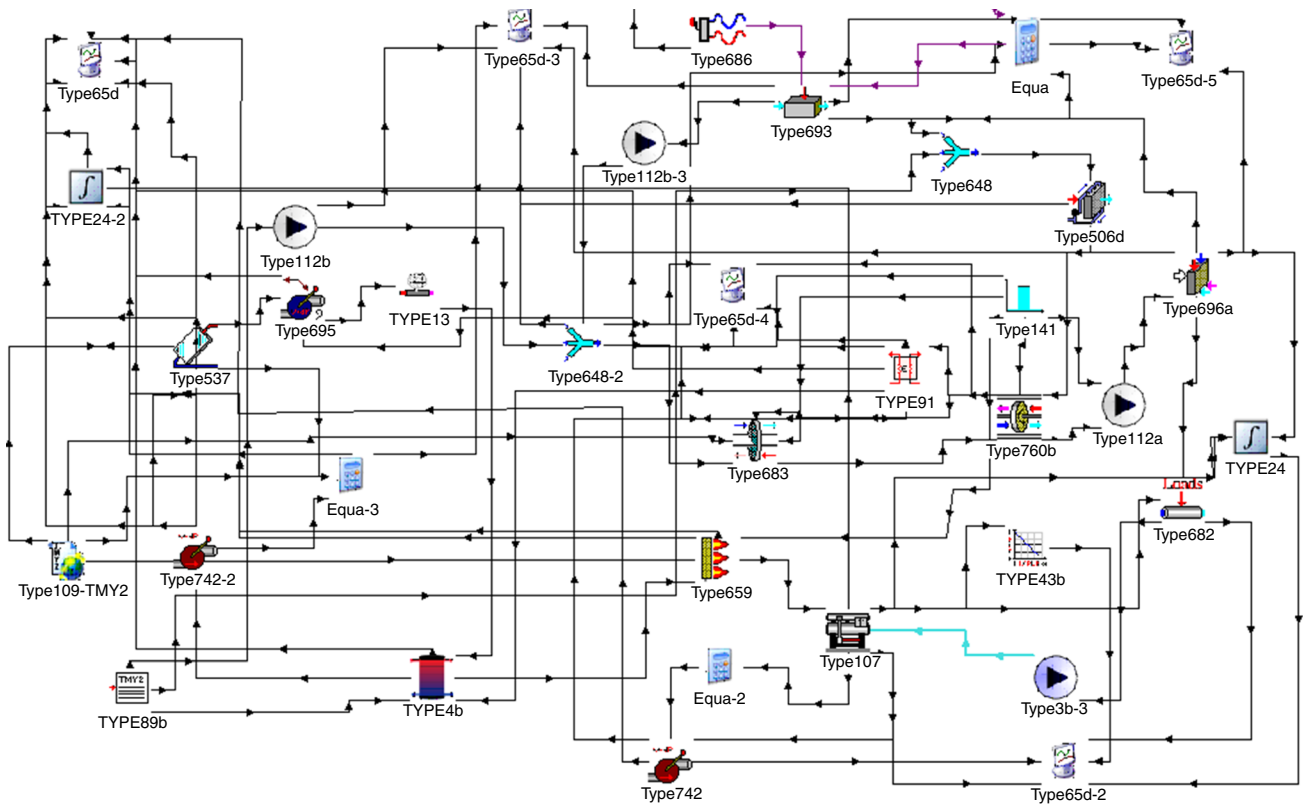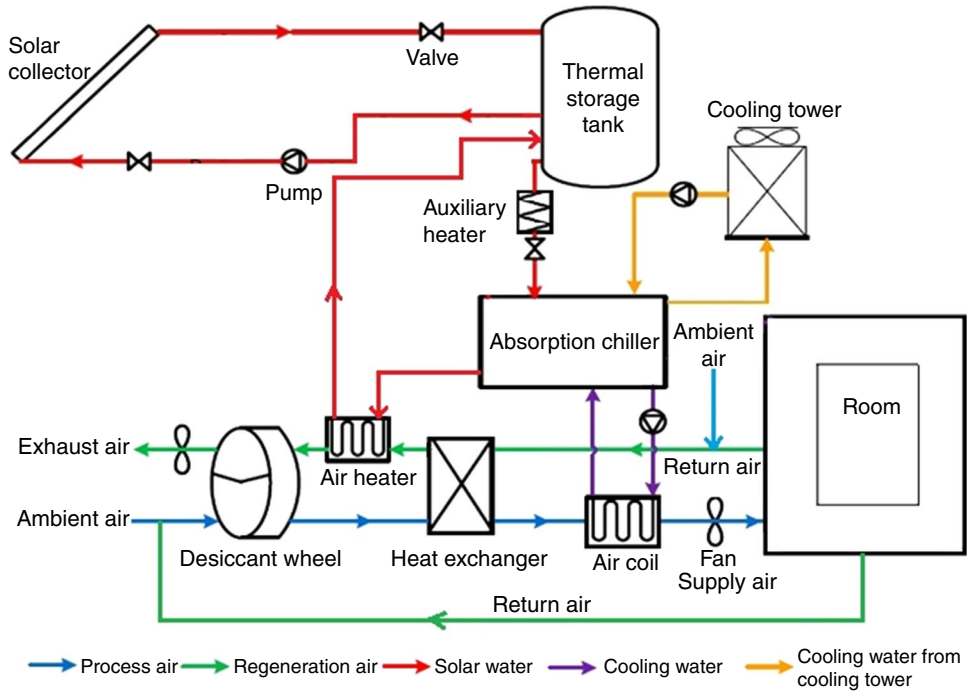

Fig. 4 The modeled plan of the third cycle in TRNSYS software

From the outlet air of type696, two outputs are taken: one goes to type693 to complete the ventilation cycle, and the other enters the chiller's size to 682. The flow of fluid from 682 in the return path as cold water enters the chiller, or the same type107. China's hot water is also provided by type537. The weather conditions of the site are simulated by type109 and entered into the input of type537, and then the heated water is pumped into 537 pumps of 695 and then the hot water enters the kettle reservoir. Typing 13 acts as a pressure relief valve in this direction and determines the amount of energy that needs to be repelled so that the temperature is always lower than the boiling time. The tank is four layers of reservoir type, and the water first enters the highest layer. After leaving the storage tank, the water enters a gas-fired furnace called type659, where it is heated up to reach the needed inlet $T = 107$. In this diagram, the type683 is the same as the slow-moving handwheel and the inlet air before it enters the type706. Typing 91 is also used as a desiccant wheel reclaimer that obtains the required heat from the chiller's hot water outlet heat.

The return water temperature from cooling coil of air handling unit (type696) was obtained according to Eq. 1:

$$T_{chw,out} = \frac{\dot{Q}_{rem}}{\dot{m} \cdot C_{Pchw}} T_{chw,set} \tag{1}$$

Then a fraction of the time of that chiller (type107) needs to function and actual capacity of chiller was obtained based on the relations 2 and 3:

$$f_{designload} = \frac{\dot{Q}_{rem}}{Capacity_{Rated}} \tag{2}$$

$$Capacity = f_{FullLoadCapacity} \times f_{NominalCapacity} \times Capacity_{Rated} \tag{3}$$

In the above equations, $Capacity_{Rated}$ is given as input by the user. Then the output cold water of the chiller enters into the cooling coil of the air handling units that have a set point of output temperature of 18 °C. In this device according to 4 and 5 equations, the latent and sensible heat of the air must be used to achieve the best output conditions.

$$\dot{Q} = \dot{m} \times (h_{in} - h_{out}) \tag{4}$$

$$\dot{Q}_{Lat} = \dot{m} \times (\omega_{in} - \omega_{out}) \tag{5}$$

In the cycle's thermal driver part, solar energy and flat panel collector (type537) are used to provide the needed hot water of the chiller due to the high radiation intensity in the project site (annual average over 22000 kWh m^{-2}). However, there is a hot water tank auxiliary and heated of gas as a backup before entering the water into chiller generator to ensure that

hot water is available 24 h a day and the temperature of the chiller input water will be 88 degrees Celsius all the time.

Collector used in the present article has a controlled pump in its output, so that the pump with changing of the output discharge always provides the temperature of 88 °C in the output, and as it is notable to provide the temperature, the discharge gets zero.

Accordingly, the collector is evaluated using Eq. 6 of the collector useful heat absorption and then Eq. 7 of fluid discharge flowing out of the collector:

$$\dot{Q}_u = A_c[F_R(\tau\alpha)I_t - F_R U_L(T_i - T_{amb})] \tag{6}$$

$$\dot{m}_{fluid} = \left(\frac{\dot{Q}}{C_p(T_i - T_{out})}\right) \tag{7}$$

That for the collector used values of $F_R(\tau\alpha)$ and $F_R U_L$ are, respectively, 0.8 and 5.0. Due to high humidity in the project site and high absolute humidity the entering into the cooling coil (0.015 kg water/kg air) and output humidity set point at 0.008 kg water/kg air, and since air handling units have been required to provide both sensible and latent loads by themselves, the energy consumption is expected to be high in this mode.

Through adding a desiccant wheel set as depicted in Fig. 4 (type653), the output air first enters into the desiccant wheel and there its absolute humidity is reduced down to 0.008. Dehumidification is done by the desiccant wheel as shown in Fig. 5 and by the $F1$ and $F2$ co-potential lines through 8 and 9 equations.

$$F1 = \frac{-2865}{T^{1.490}} + 4.344\omega \tag{8}$$

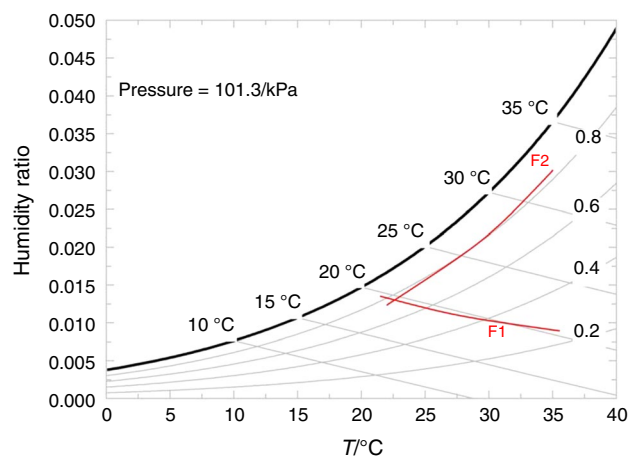$$F2 = T1.490 - 1.127\omega0.07969 \tag{9}$$

Fig. 5 $F1$ and $F2$ co-potential lines for silica gel

In the following process, a heat wheel exchanger (type760b) is posited for the purpose of heat and energy regeneration from returning air inside the building, that in fact has been an eddy air exchanger and itself has led to more decrease in sensible heat.

Minimum heat capacity, enthalpy of the air at the outlet of this device and the sensible heat content between exchanged two streams are obtained, respectively, through 10–12.

$$C_{min} = min(\dot{m}_{exh}C_{Pexh}, \dot{m}_{fresh}C_{Pfresh})$$ (10)

$$\dot{Q}_{sens} = \varepsilon_{sens}C_{min}(T_{exh,in} - T_{fresh,in})$$ (11)

$$h_{fresh,out} = h_{fresh,in} + \frac{\dot{Q}_{sens}}{\dot{m}_{fresh}}$$ (12)

On the back track as well, the air after flowing within the heat exchanger to reach the required temperature for recovery desiccant wheel and as the result of doing continuous and accurate dehumidification measurement may pass through the two paths or, according to Fig. 3, enters directly into gas heaters and then into the desiccant wheel on the circumstances according to Eq. 13.

$$h_{air,out} = h_{air,in} + \frac{q_{in}}{\dot{m}} - \frac{UA}{\dot{m}}(\bar{T} - T_{amb})$$ (13)

Or according Fig. 4 and the optimized cycle enters into a water-to-air exchanger (type91) and is heated by the returning hot water from the chiller generator, and then enters into the desiccant wheel. By this, the direct heater for the regeneration air is no more required and this causes to save energy and cost.

Economic analysis

The economic analysis of solar systems uses a variety of methods and criteria which includes Life Cycle Cost (LCC), Life Cycle Saving (LCS), Payback Time (PT) and Return on Investment (ROI).

In this paper, LCC method is used to estimate the cost of each system. According to this method, the total current and fixed costs of the system can be calculated during the period of operation. The initial cost of the solar system is obtained through relation 14.

$$Cs = C_A A_G + C_v V_s + C_E$$ (14)

where C_E is equal to 12% of collector and tank costs. The fuel current cost per 1 month is calculated through relation 15 and per year through relation 16.

$$C_{aux} = day \times \frac{Q_{aux}}{L_v} \times C_g$$ (15)

$$C_{auxY} = \sum_{i=1}^{12} C_{aux}$$ (16)

The point that should be noted here is that the current prices were paid during the years of unit operation, while the initial cost is paid in the first year. Therefore, different year's costs ought to be calculated in the rate of the first year so that they can be sum up. For this purpose, a factor called the present worth factor is used which can be calculated using Eq. 17:

$$PWF(N, I, d) = \sum_{j=1}^{N} \frac{(1+i)^{j-1}}{(1+d)^j} = \begin{cases} \frac{1}{d-i}\left[1-(\frac{1+i}{1+d})N\right] & \text{if}(i \neq d) \\ \frac{N}{1+i} & \text{if}(i=d) \end{cases} \longrightarrow$$ (17)

In the above equation, N is number of year's number of the system lifetime, i is inflation rate, and d is the discount rate. On this basis and in accordance with relations 18 and 19, the total cost of each system is calculated separately in the rate of the first year and the superior cycle introduced from the economic perspective.

$$C_{auxT} = C_{auY} \times PWF(N, i, d)$$ (18)

$$LCC = C_s + C_{auxT}$$ (19)

In the economic analysis of systems in the present study, the following hypothesis has been considered:

- The market discount rate equal to 20%.
- The market inflation rate equal to 20% and fuel price inflation rate equal to 15%.
- Number of years for system performance equal to 20.
- The whole system at the end of a 20-year period was sold to the rate of 50% of its initial price.
- The entire solar sector of each system including collector and storage tank are provided with loans funded for 15% interest and 20-year repay.
- The cost of the equipment electricity consumption is neglected.
- The efficiency of the whole cycle during the functioning year does not change.

Results

It was noted in the previous section that the above modeling has been developed for a computer building in Bandar Abbas, Iran, with 400 meters of area and population occupation. Type of the used collector was also flat with an area of 300 square meters and the storage tank was of multi-node

Table 2 Results of the cycles modeling

	System 1	System 2	System 3
Cooling load per year, kJ	1,520,000,000	894,000,000	880,000,000
Chiller capacity, t	42	31	29
Annual energy consumption of auxiliary heater	8,470,000,000	6,400,000,000	6,000,000,000
Collector useful heat gain per year, kJ	750,000,000	750,000,000	810,000,000
Cost of the whole system during the 20 years in the rate of the first year per cubic meter 0.016$	234,314	230,271	226,526
Cost of the whole system during the 20 years in the rate of the first year per cubic with the price of 0.28$ per cubic meter	862,838	741,867	701,171

Fig. 6 Comparison between the basic parameters in cycles
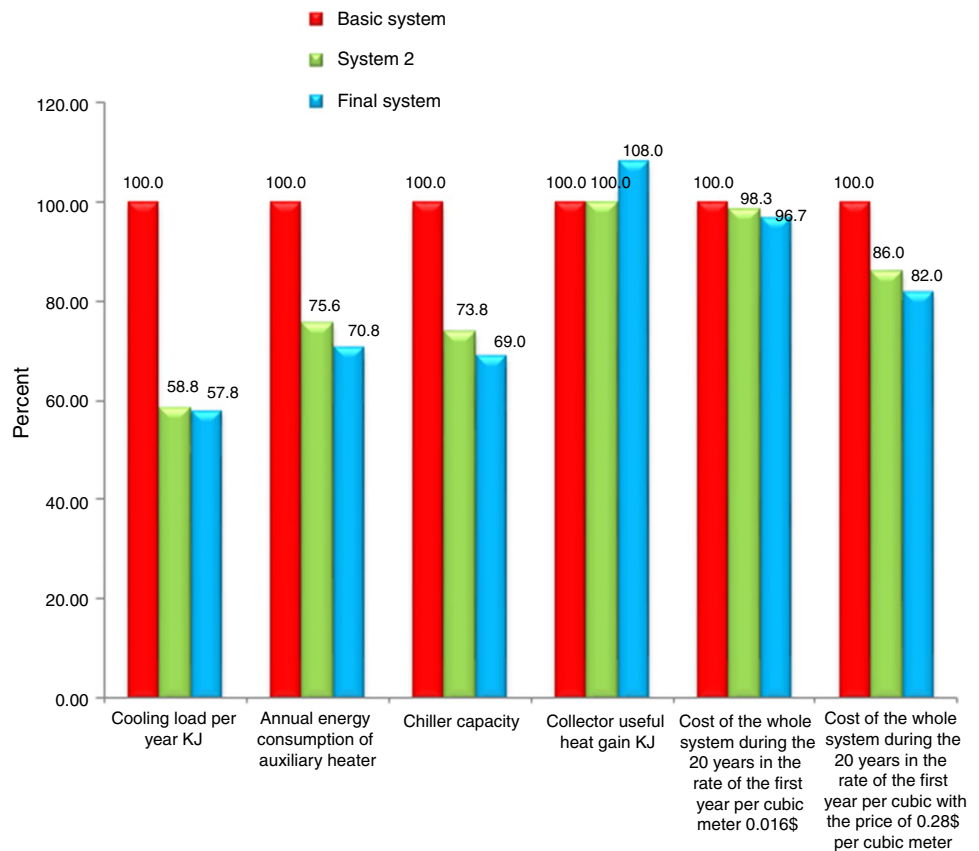
type to the total volume of 12 m^3. According to the modeling system in TRNSYS and analysis of the output parameters, results of this modeling are given in Table 2.

In estimating the system gas consumption prices, the sales price per 1 m^3 of natural gas is considered to be equal to 0.28 $ based on the general policy of the state and due to the gradual elimination of energy subsidies. Therefore, for clear understanding of the issue, the economic analysis once is done with the current price of natural gas (0.016 $ per cubic meter) and another time on the basis of the intended final price.

Figures 6 and 7 also, in a more clear way, show comparison of three cycles. In this diagram, the parameters of basic cycle are considered 100%, and other related parameters of the 2 other cycles have been measured in percentage.

As can be seen in Fig. 6, the cooling load imposed on the third cycle as the result of the optimization cycle dropped to 42.2% compared to the base cycle and to 1% compared to the second cycle. Also, the energy content needed in auxiliary heaters, as expected, in the third cycle dropped to 29% compared to the base cycle and to 4.6% compared to the second cycle. On the other hand, as in the basic and second cycles
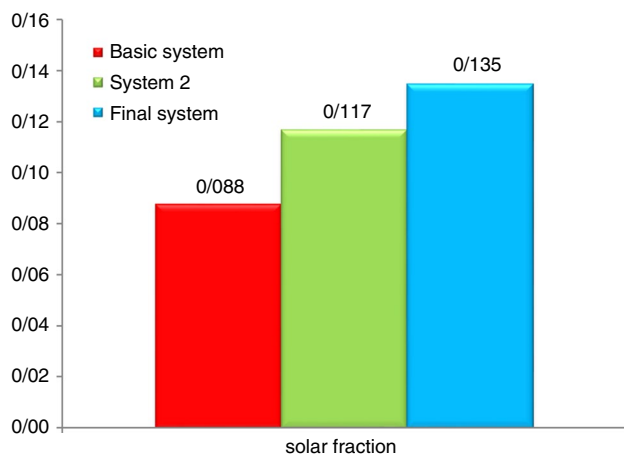
Fig. 7 Comparison between the basic parameters in cycles (solar fraction)

the water temperature entering into the collector is the same, so the collector useful heat gain in these two cycles is the fixed value of 750,000,000 kJ, while considering drop of this temperature in the third cycle, this parameter is increased to 8% compared to the two previous cycles which is a significant amount.

After cooling load reduction of the cycles 2 and 3, the chiller absorption capacity used in the third cycle dropped to 31% compared to the base cycle and to 4.8% compared to the second cycle. However, regarding the reduction in energy consumption by auxiliary gas heaters, it has been observed that the natural gas consumption over 20 years of system functioning in the third cycle dropped to the rate of 29% compared to the basic cycle and to the rate of 4.6% compared to the second cycle that is very desirable due to the limited energy resources and the environmental impact.

Finally, after economic analysis of the three cycles based on costs method over the lifetime and according to Fig. 6, it can be seen, including the price of gas as 0.016 $ per cubic meter, the total cost of the third cycle dropped to the rate of 3.3% compared to the basic cycle and 1.7% compared to the second cycle. However, with the final intended price for natural gas, namely 0.28 $ per cubic meter, the third cycle total cost dropped to the rate of 18% (equivalent to 6.58 billion Rials) compared to the first cycle and 4% (equivalent to 35,695 $) compared to the second cycle reduced.

Conclusions

According to the diagram in Fig. 6 and Table 2, parameters related to energy consumption, fuel, and costs have taken a decreasing trend from the first to the third cycle, which is desirable. The uptake of collector useful heat has a direct impact on collector efficiency and the solar part of

the cycles. In cycles 1 and 2, due to the equal collector inlet water temperature, the value is constant, but in the third cycle due to the use of water returning from the chiller desiccant wheel in the regeneration process, this value increased which is also useful. Consequently, the third cycle with 1,371,980 m^3 of natural gas savings and 156,667 $ cost savings compared to basis cycle was selected as the most optimal cycle, both environmentally and economically.

References

1. Lucas L. Iir news. Int J Refrig. 1998;21(2):87–8.
2. Jaber JO, Badran OO, Abu-Shikhah N. Sustainable energy and environmental impact: role of renewables as clean and secure source of energy for the 21st century in Jordan. Clean Technol Environ Policy. 2004;6(3):174–86.
3. Florides GA, Kalogirou SA, Tassou SA, Wrobel LC. Modeling, simulation and warming impact assessment of a domestic-size absorption solar cooling system. Appl Therm Eng. 2002;22(12):1313–25.
4. Daou K, Wang R, Xia Z. Desiccant cooling air conditioning: a review. Renew Sustain Energy Rev. 2006;10(2):55–77.
5. Farshad SA, Sheikholeslami M. Nanofluid flow inside a solar collector utilizing twisted tape considering exergy and entropy analysis. Renew Energy. 2019;141:246–58.
6. Sheikholeslami M, Gerdroodbary MB, Shafee A, Tlili I. Hybrid nanoparticles dispersion into water inside a porous wavy tank involving magnetic force. J Therm Anal Calorim. 2019. https://doi.org/10.1007/s10973-019-08858-6.
7. Szilágyi IM, Kállay-Menyhárd A, Šulcová P, Kristóf J, Pielichowski K, Šimon P. Recent advances in thermal analysis and calorimetry presented at the 1st journal of thermal analysis and calorimetry conference and 6th V4 (Joint Czech-Hungarian-Polish-Slovakian) thermoanalytical conference (2017). J Therm Anal Calorim. 2018;133:1–4.
8. Yang L, Ji W, Zhang Z, Jin X. Thermal conductivity enhancement of water by adding graphene nano-sheets: consideration of particle loading and temperature effects. Int Commun Heat Mass Transf. 2019;109:104353.
9. Sheikholeslami M, Sheremet MA, Shafee A, Li Z. CVFEM approach for EHD flow of nanofluid through porous medium within a wavy chamber under the impacts of radiation and moving walls. J Therm Anal Calorim. 2019. https://doi.org/10.1007/s10973-019-08235-3.
10. Sheikholeslami M, Arabkoohsar A, Jafaryar M. Impact of a helical-twisting device on nanofluid thermal hydraulic performance of a tube. J Therm Anal Calorim. 2019. https://doi.org/10.1007/s10973-019-08683-x.
11. Sheikholeslami M. New computational approach for exergy and entropy analysis of nanofluid under the impact of Lorentz force through a porous media. Comput Methods Appl Mech Eng. 2019;344:319–33.
12. Sheikholeslami M, Haq R-U, Shafee A, Li Z, Elaraki YG, Tlili I. Heat transfer simulation of heat storage unit with nanoparticles and fins through a heat exchanger. Int J Heat Mass Transf. 2019;135:470–8.
13. Sheikholeslami M, Haq RU, Shafee A, Li Z. Heat transfer behavior of nanoparticle enhanced PCM solidification through an enclosure with V shaped fins. Int J Heat Mass Transf. 2019;130(2019):1322–42.

14. Qin Y. A review on the development of cool pavements to mitigate urban heat island effect. Renew Sustain Energy Rev. 2015;52:445–59.

15. Sheikholeslami M, Shehzad SA, Li Z, Shafee A. Numerical modeling for alumina nanofluid magnetohydrodynamic convective heat transfer in a permeable medium using Darcy law. Int J Heat Mass Transf. 2018;127:614–22.

16. Qin Y, He Y, Hiller JE, Mei G. A new water-retaining paver block for reducing runoff and cooling pavement. J Clean Prod. 2018;199:948–56.

17. Sheikholeslami M, Ghasemi A, Li Z, Shafee A, Saleem S. Influence of CuO nanoparticles on heat transfer behavior of PCM in solidification process considering radiative source term. Int J Heat Mass Transf. 2018;126:1252–64.

18. Qin Y, Luo J, Chen Z, Mei G, Yan L-E. Measuring the albedo of limited-extent targets without the aid of known-albedo masks. Sol Energy. 2018;171:971–6.

19. Qin Y, Liang J, Luo Z, Tan K, Zhu Z. Increasing the southern side-slope albedo remedies thermal asymmetry of cold-region roadway embankments. Cold Reg Sci Technol. 2016;123:115–20.

20. Fong KF, Chow TT, Lee CK, Lin Z, Chan LS. Comparative study of different solar cooling systems for buildings in subtropical city. Sol Energy. 2010;84(2):227–44.

21. Gebreslassie BH, Guillén-Gosálbez G, Jiménez L, Boer D. Solar assisted absorption cooling cycles for reduction of global warming: a multi-objective optimization approach. Solar Energy. 2012;86:2083–94.

22. Henning H-M, Erpenbeck T, Hindenburg C, Santamaria IS. The potential of solar energy use in desiccant cooling cycles. Int J Refrig. 2001;24:220–9.

23. Daou K, Wang RZ, Xia ZZ. Desiccant cooling air conditioning: a review. Renew Sustain Energy Rev. 2006;10:55–77.

24. Krishna S, Murthy SS. Experiments on silica gel rotary dehumidifier. Heat Recovery Syst CHP. 1989;9(467–473):1989.

25. Vineyard EA, Sand JR, Durfee DJ. Performance characteristics for a desiccant system at two extreme ambient conditions. ASHRAE Trans. 2002;108:587–96.

26. Sheikholeslami M, Darzi M, Li Z. Experimental investigation for entropy generation and exergy loss of nano-refrigerant condensation process. Int J Heat Mass Transf. 2018;125:1087–95.

27. Sheikholeslami M, Ghasemi A. Solidification heat transfer of nanofluid in existence of thermal radiation by means of FEM. Int J Heat Mass Transf. 2018;123:418–31.

28. Qin Y, Zhao Y, Chen X, Wang L, Li F, Bao T. Moist curing increases the solar reflectance of concrete. Constr Build Mater. 2019;215:114–8.

29. Sheikholeslami M, Shehzad SA. CVFEM simulation for nanofluid migration in a porous medium using Darcy model. Int J Heat Mass Transf. 2018;122:1264–71.

30. Sheikholeslami M, Shehzad SA. Simulation of water based nanofluid convective flow inside a porous enclosure via non-equilibrium model. Int J Heat Mass Transf. 2018;120:1200–12.

31. Qin Y, He H, Ou X, Bao T. Experimental study on darkening water-rich mud tailings for accelerating desiccation. J Clean Prod. 2019. https://doi.org/10.1016/j.jclepro.2019.118235.

32. Sheikholeslami M. Numerical approach for MHD Al_2O_3-water nanofluid transportation inside a permeable medium using innovative computer method. Comput Methods Appl Mech Eng. 2019;344:306–18.

33. Sheikholeslami M, Seyednezhad M. Simulation of nanofluid flow and natural convection in a porous media under the influence of electric field using CVFEM. Int J Heat Mass Transf. 2018;120:772–81.

34. Sheikholeslami M, Rokni HB. Numerical simulation for impact of Coulomb force on nanofluid heat transfer in a porous enclosure in presence of thermal radiation. Int J Heat Mass Transf. 2018;118:823–31.

35. Yang L, Mao M, Huang JN, Ji W. Enhancing the thermal conductivity of SAE 50 engine oil by adding zinc oxide nano-powder: an experimental study. Powder Technol. 2019;356:335–41.

36. Sheikholeslami M, Bhatti MM. Active method for nanofluid heat transfer enhancement by means of EHD. Int J Heat Mass Transf. 2017;109:115–22.

37. Yang L, Ji W, Huang JN, Xu G. An updated review on the influential parameters on thermal conductivity of nano-fluids. J Mol Liq. 2019;296:111780.

38. Sheikholeslami M, Ellahi R. Three dimensional mesoscopic simulation of magnetic field effect on natural convection of nanofluid. Int J Heat Mass Transf. 2015;89:799–808.

39. Yang L, Xu J, Du K, Zhang X. Recent developments on viscosity and thermal conductivity of nanofluids. Powder Technol. 2017;317:348–69.

40. Sheikholeslami M. Magnetic field influence on CuO–H_2O nanofluid convective flow in a permeable cavity considering various shapes for nanoparticles. Int J Hydrog Energy. 2017;42:19611–21.

41. Vo DD, Hedayat M, Ambreen T, Shehzad SA, Sheikholeslami M, Shafee A, Nguyen TK. Effectiveness of various shapes of Al_2O_3 nanoparticles on the MHD convective heat transportation in porous medium: CVFEM modeling. J Therm Anal Calorim. 2019. https://doi.org/10.1007/s10973-019-08501-4.

42. Yang L, Du K. A comprehensive review on the natural, forced and mixed convection of non-Newtonian fluids (nanofluids) inside different cavities. J Therm Anal Calorim. 2019. https://doi.org/10.1007/s10973-019-08987-y.

43. Sharaf MA, Nafey AS, García-Rodríguez L. Exergy and thermo-economic analyses of a combined solar organic cycle with multi effect distillation (MED) desalination process. Desalination. 2011;272:135–47.

44. Montes MJ, Abánades A, Martínez-Val JM, Valdés M. Solar multiple optimization for a solar-only thermal power plant, using oil as heat transfer fluid in the parabolic trough collectors. Sol Energy. 2009;83:2165–76.